ADVANCED BIOSYSTEMS
www.adv-biosys.com

Optogenetically Controlled TrkA Activity Improves the Regenerative Capacity of Hair-Follicle-Derived Stem Cells to Differentiate into Neurons and Glia

Taida Huang, Yan Zhang, Zitian Wang, Yunxin Zeng, Nan Wang, Huaxun Fan, Zhangsen Huang, Yixun Su, Xiaomin Huang, Hui Chen, Kai Zhang, and Chenju Yi**

Hair-follicle-derived stem cells (HSCs) originating from the bulge region of the mouse vibrissa hair follicle are able to differentiate into neuronal and glial lineage cells. The tropomyosin receptor kinase A (TrkA) receptor that is expressed on these cells plays key roles in mediating the survival and differentiation of neural progenitors as well as in the regulation of the growth and regeneration of different neural systems. In this study, the OptoTrkA system is introduced, which is able to stimulate TrkA activity via blue-light illumination in HSCs. This allows to determine whether TrkA signaling is capable of influencing the proliferation, migration, and neural differentiation of these somatic stem cells. It is found that OptoTrkA is able to activate downstream molecules such as ERK and AKT with blue-light illumination, and subsequently able to terminate this kinase activity in the dark. HSCs with OptoTrkA activity show an increased ability for proliferation and migration and also exhibited accelerated neuronal and glial cell differentiation. These findings suggest that the precise control of TrkA activity using optogenetic tools is a viable strategy for the regeneration of neurons from HSCs, and also provides a novel insight into the clinical application of optogenetic tools in cell-transplantation therapy.

1. Introduction

Different types of stem cells are being widely investigated in cell-transplantation and regenerative therapies for neural defects caused by congenital and acquired pathologies.[1–4] However, the route to the clinic for such cell-based therapies is a long one due to prevalent issues such as alloimmune rejection, the availability of cell sources and the potential long-term risk for tumorigenesis.[4–6] Hair follicles are an easily accessible structure on the skin and the stem cells harbored within them can consistently undergo self-renewal.[7,8] Hair-follicle-derived stem cells (HSCs) isolated from the bulge region of hair follicles were able to differentiate into neuronal and glial cells in vitro and also regenerate neurons in animal recipients.[8–10] HSCs are an ideal cell source for neural regeneration not only due to its differentiation potency to neural cell types, but also its reduced tumorigenicity as somatic stem cells, easy accessibility, as well as its lower rate for immunologic rejection during autologous transplantation.

Neurotrophin signaling is a key process that determines neural stem cell function, influencing cell survival, cell division and differentiation. These effects carry on to modulate functions in fate-determined cells, such as axonal and dendritic growth of neurons, cell death, neurotransmitter secretion, and neuronal activity.[11] Neurotrophin signaling is traditionally mediated through ligand binding to the tropomyosin receptor kinase (Trk) receptor tyrosine kinase family and, with less affinity, to the p75 neurotrophin receptor ($p75^{NTR}$).[11–13] Although Trk

Dr. T. Huang, Y. Zeng, N. Wang, Dr. Z. Huang, Dr. Y. Su, X. Huang, Prof. C. Yi
The Seventh Affiliated Hospital of Sun Yat-sen University
Shenzhen 518107, China
E-mail: yichj@mail.sysu.edu.cn
Dr. Y. Zhang
Department of Orthopedics
Tianjin Medical University General Hospital
Tianjin 300052, China
Dr. Z. Wang
Tsinghua-Berkeley Shenzhen Institute
Tsinghua University
Shenzhen 518055, China
The ORCID identification number(s) for the author(s) of this article can be found under https://doi.org/10.1002/adbi.202000134.
H. Fan, Prof. K. Zhang
Department of Biochemistry
School of Molecular and Cellular Biology
University of Illinois at Urbana-Champaign
Urbana, IL 61801, USA
E-mail: kaizkaiz@illinois.edu
Prof. H. Chen
School of Life Sciences
Faculty of Science
University of Technology Sydney
PO Box 123, Broadway, NSW 2007, Australia

DOI: 10.1002/adbi.202000134

receptors have been investigated in a variety of different cell types, little is known about its function in HSCs during neural differentiation. As key Trk-mediated effects such as active proliferation, cellular migration, and differentiation are critical processes in cell graft survival and its ability to fully regenerate neurons after transplantation, various groups have examined the effect of Trk receptors activation in a variety of neural progenitors by using techniques such as genetic overexpression or by agonist-induced activation of the receptor.[13–15] However, these approaches are not feasible for clinical applications. One major issue is that certain receptors such as TrkC can act as an oncogene in a variety of tumor cells, and manipulation of *TrkC* overexpression using genetic methods has been acknowledged to result in an extremely high tumorigenic potential. Furthermore, manipulation of exogenous Trk activity using such methods results in receptor levels persisting in a non-physiological manner even after neuronal differentiation. Also, using small-molecule agonists of Trk receptors has its own caveats; a plethora of unknown off-target effects suggests that rigorous testing before clinical use will be required.[16,17] Therefore, strategies that can enact precise control on the activities of Trk receptors in HSCs such as through some form of "biochemical switch" need to be developed in order to manipulate neural regeneration efficiency in these cells, with the condition that such a switch must be able to terminate Trk activity after regeneration processes to ensure that levels of Trk receptors can be restored to physiological levels after fate determination.

Emerging cutting-edge optogenetic techniques allow for spatiotemporal regulation of the activity of single molecules.[18–21] Previously, we developed an optogenetic tool (OptoTrkA) that allows reversible activation of tropomyosin receptor kinase A (TrkA) signaling by the fusion of the intracellular domain of TrkA (TrkA-ICD) with the light–oxygen–voltage domain of aureochrome 1 from *Vaucheria frigida* (AuLOV).[18] We expect that OptoTrkA is only activated after excitation by light and this activation is spontaneously resolved in the dark and activation of TrkA using the OptoTrkA system will influence the proliferation, migration, and neural differentiation (to neuronal and glial cell types) of HSCs.

In this study, we used the OptoTrkA system within primary cultured HSCs isolated from mouse vibrissa hair follicles and found that light-induced TrkA activity was able to promote cell proliferation, migration, and differentiation into neuronal and glial cells in vitro. The results of our study demonstrated the optogenetically controlled TrkA activity in HSCs and revealed the functional role of TrkA in driving the neurogenesis of HSCs.

2. Results

2.1. Optogenetic Activation of TrkA in HSCs

Previously, we developed an optogenetic system (OptoTrkA) that allows for TrkA activation upon controlled light excitation (**Figure 1**A,B). This system was constructed by fusing the intracellular domain of TrkA (TrkA-ICD) with the light–oxygen–voltage domain of *V. frigida* aureochrome 1 (AuLOV). Upon light excitation, the homo-association of AuLOV pulls two copies of TrkA-ICD within close proximity and further initiating its cross- and autophosphorylation (Figure 1B). HSCs originated from bulge region of mouse vibrissa hair follicle were primary cultured in vitro and transfected with the plasmid expressing OptoTrkA (Figure 1C). HSCs with OptoTrkA transfection were subjected to cellular analyses, including BrdU staining, wound healing assay, directed differentiation analysis, etc. in order to determine the functional effects of TrkA on the proliferation, migration, and neural differentiation of HSCs (Figure 1D).

2.2. Isolation and Characterization of HSCs

Mouse vibrissa hair follicle explants were isolated according to the procedure as described in the methods (**Figure 2**A, i–iv). After the culture of mouse follicle explants, we found that proliferative cells migrate outward from the explant in migration medium after 2–3 days, whereupon the explant was removed on Day 4 (Figure 2B). In general, we found that cell numbers ranged from between 8000 and 10 000 per explant when cultured in expansion medium on Day 7 whereupon these cells were enzymatically dissociated for passaging (Figure 2B). Characterization of primary cultured cells was performed by immunofluorescence staining of markers such as Nestin, p75, Sox10, and Oct4. We found that early migrated cells (Day 3) expressed markers such as Nestin, p75, and Sox10 (Figure 2C). After passaging, sub-cultured cells were found to also be Nestin and Oct4 double immunoreactive (Figure 2D). In addition, we isolated mRNA from these cells and were able to detect the expression of stem cell markers such as *Oct4*, *Sox2*, and *Nanog* by reverse-transcription PCR (Figure 2E). Meanwhile, we also found that expression of neural stem cell markers, including *Nes* (encoding Nestin) *Sox9*, *Sox10*, and *Ngfr* (encoding $p75^{NTR}$), were also found to be expressed in these cells (Figure 2E). In summary, the cells isolated from mouse vibrissa hair follicle exhibited markers of stem cells, especially neural stem cells, which were similar to the HSCs reported previously;[7,9,10] thus, we also termed these cells as HSCs in our present study.

3. Light-Stimulated OptoTrkA Activity Enhances the Proliferation and Migration of HSCs

Previous studies have reported that TrkA selectively promotes cell proliferation and migration or may even result in cell death pathway activation in a variety of cell types.[16,22–24] To determine whether blue-light-induced OptoTrkA activity has any effect on the proliferation and migration of HSCs, we introduced OptoTrkA into primary cultured HSCs. This was followed by BrdU staining to examine proliferation and a wound healing assay to examine cellular migration. HSCs with light-induced activation of OptoTrkA (pOptoTrkA-light) showed a significantly higher percentage of BrdU immunoreactivity as compared with those HSCs in pEGFP-dark, pOptoTrkA, and pOptoTrkA-dark groups, which suggests that activation of OptoTrkA was able to increase the proliferation of HSCs (**Figure 3**A, B). In the wound healing assay, HSCs with blue-light-activated OptoTrkA showed

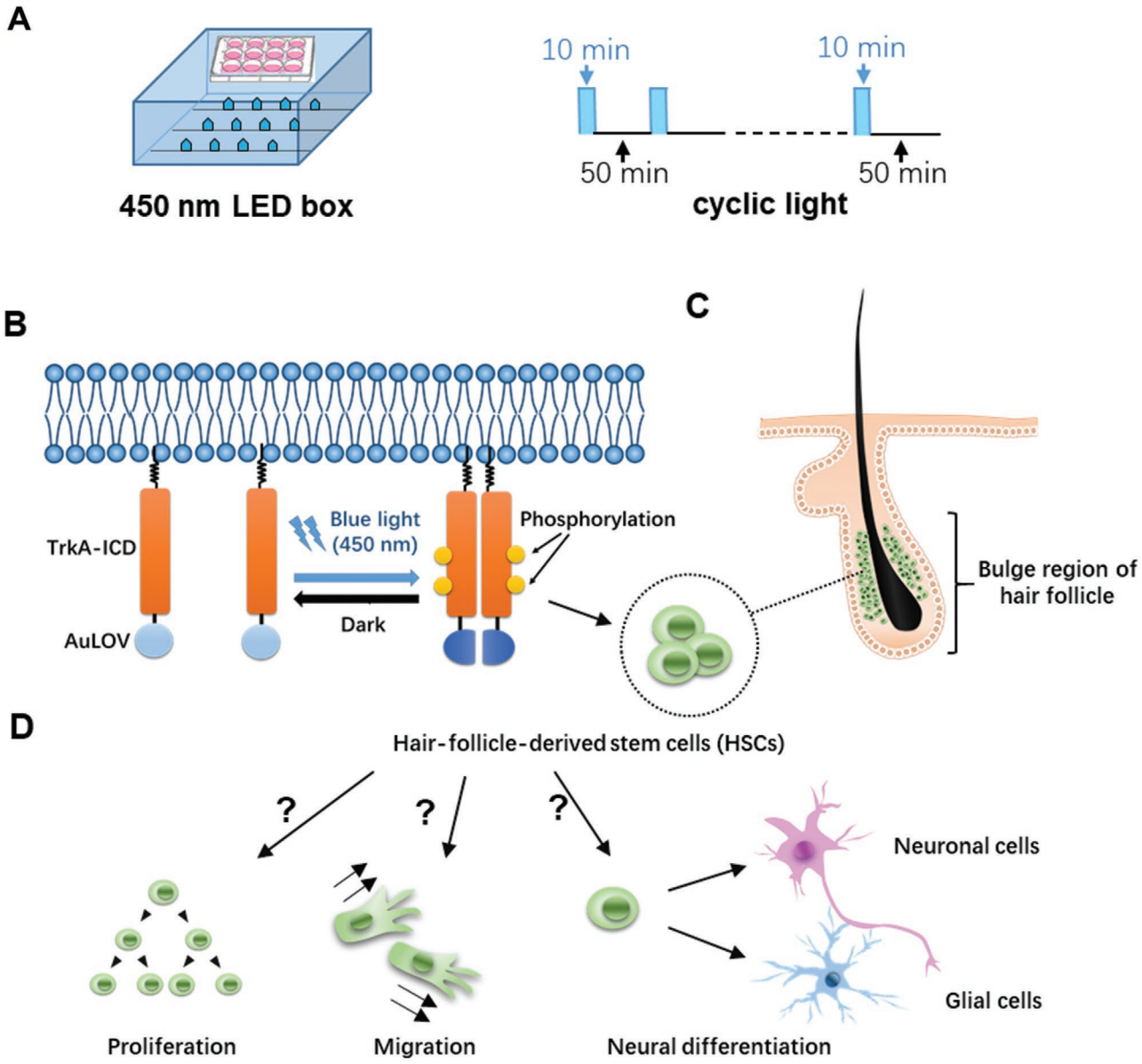

Figure 1. Schematic illustration of activation of OptoTrkA in HSCs. A) OptoTrkA-transfected HSCs and control HSCs were cultured in a 12-well plate which was placed on the LED light box. Light illumination was set to a 10-min-on, 50-min-off cycle. B) HSCs were isolated from the bulge region of mouse vibrissa hair follicles. C) Upon blue-light illumination, the photosensitive protein, AuLOV dimerizes TrkA-ICD, which leads to activation of TrkA signaling as detected by autophosphorylation. D) The function of OptoTrkA in regulating the proliferation, migration, and neural differentiation of HSCs was investigated in this study.

a significantly higher ability to migrate into the wound over a period of 12 and 24 h when compared to the other three control groups (Figure 3C,D). By counting the average distance between each cell to its closest neighbor at the 24 h time point, we found that HSCs were more dispersed in the light-activated OptoTrkA group as compared to the cells in other groups (Figure 3E). We also performed the TUNEL assay and Caspase-3 staining of HSCs with and without OptoTrkA activity and found no significant difference in cell apoptosis or cell death (Supporting Information figures). These gain-of-function studies of OptoTrkA therefore suggest that the proliferation and migration of HSCs could be enhanced by the light-induced activation of OptoTrkA in vitro.

4. Light-Induced Activation of OptoTrkA Can Boost Neuronal Cell Differentiation of HSC

To determine whether activated OptoTrkA can improve HSC neuronal cell differentiation, we performed a directed differentiation protocol followed by immunofluorescence staining of neuronal markers. pOptoTrkA was transfected into primary

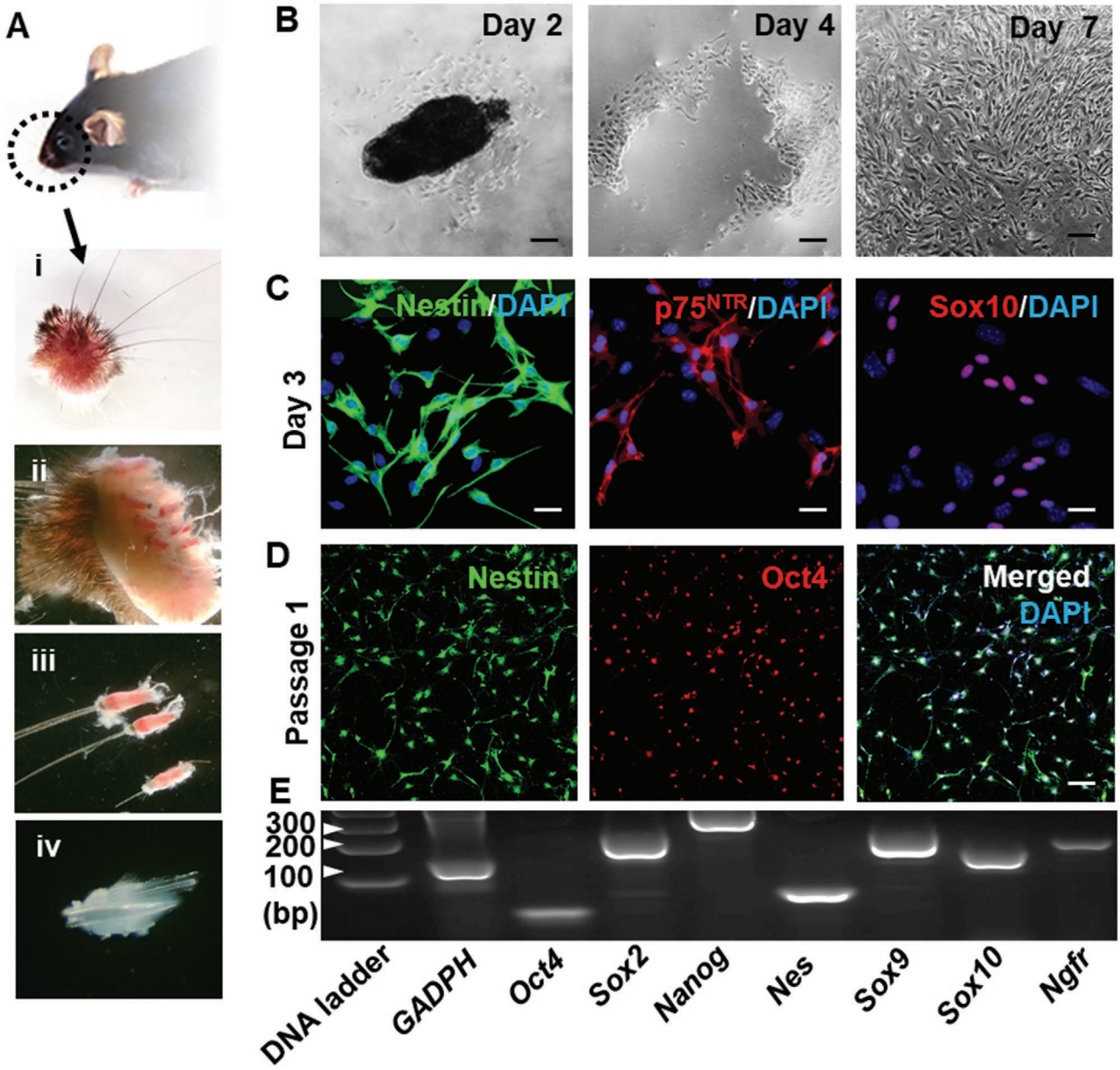

Figure 2. Primary culture of HSCs from hair follicle explant. A) The whisker pads of the adult mouse were i) dissected and ii) placed in PBS under a stereoscopic microscope. iii) Single hair follicles are then isolated. iv) A single bulge explant for culture was obtained by removing the connective tissue capsule. B) The explant isolated from the mouse vibrissa hair follicles of postnatal mice is cultured on collagen type I-coated coverslips. The HSCs migrate from hair follicle explant on approximately Day 2 and the explant was removed on Day 4. Hereafter, the HSCs population was expanded for a subsequent 3 days before passaging. Scale bar: 200 µm. C) After the bulge explants were removed, the cells were stained for the expression of Nestin, Sox10, and $p75^{NTR}$. Scale bar: 20 µm. D) After sub-culturing, HSCs were found to be Nestin and Oct4 double immunoreactive. Scale bar: 100 µm. E) The expression of *Oct4*, *Sox2*, *Nanog*, *Nes*, *Sox9*, *Sox10*, and *Ngfr* was determined by reverse-transcription PCR.

cultured HSCs, and these HSCs were induced into neurons in neuronal cell differentiation medium. By examining neuronal markers Tuj1, PGP9.5, and Map2, we found that all the HSCs in four different groups were able to differentiate into neurons (**Figure 4**A,D and Figure 1A, Supporting Information). However, the activated OptoTrkA group had a significantly higher percentage of Tuj1 and PGP9.5 immunoreactive cells as compared to those in the control groups (Figure 4B,E). To further confirm that activation of OptoTrkA can promote neuronal cell differentiation, we analyzed the number of neuronal cells, which showed a fibrous cell structure. We found that the HSCs with activated OptoTrkA were able to show a higher percentage of cells with fibrous morphology as compared to the controls (Figure 4C,F). These findings reveal that OptoTrkA not only promotes the neuronal differentiation of HSCs but also can accelerate the maturation of neuronal cells.

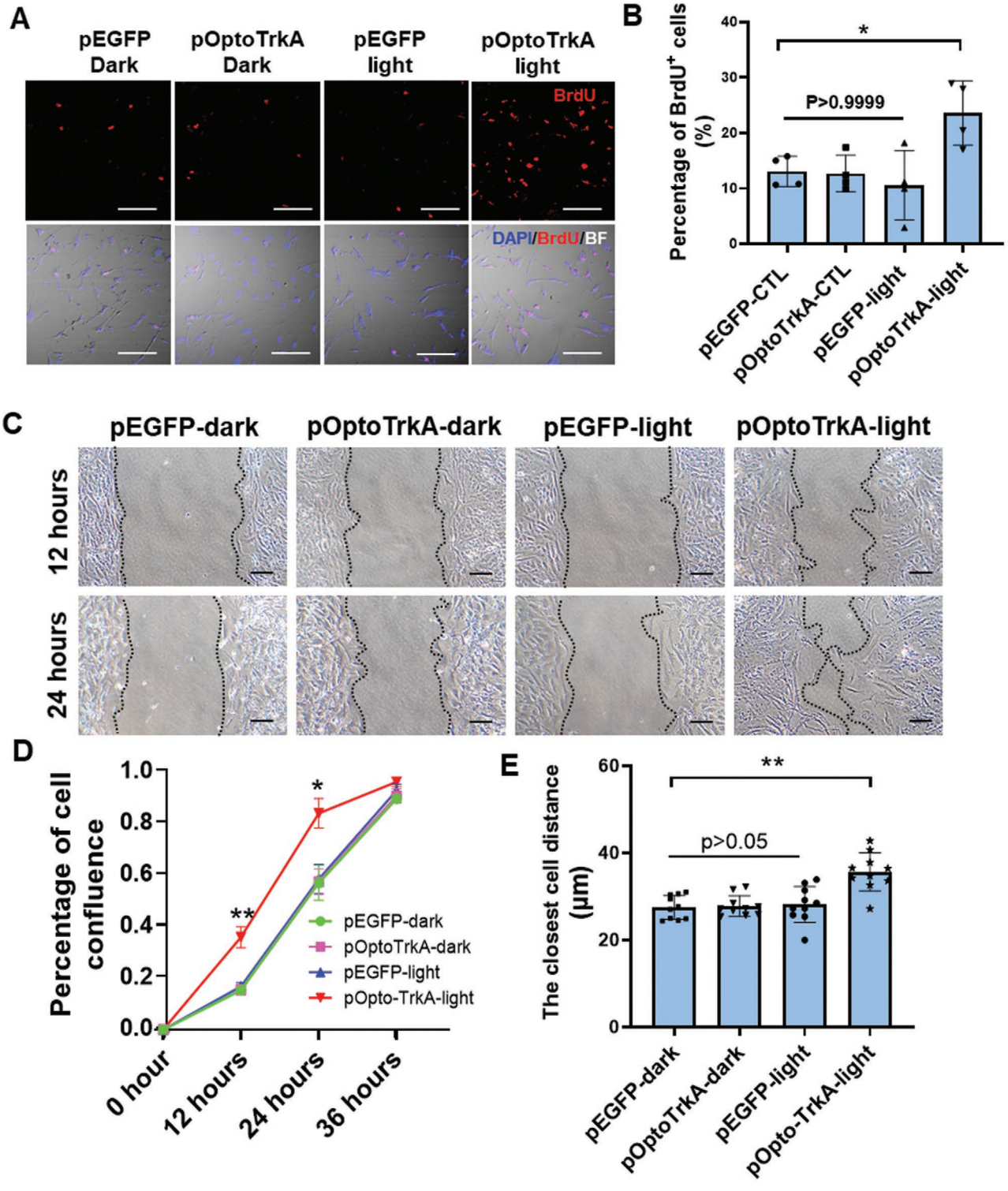

Figure 3. Light-induced activation of OptoTrkA promotes proliferation and migration of HSCs. A) Immunofluorescence staining of BrdU in OptoTrkA-transfected HNCSs and sham-transfected HNCSs with or without continuous 12 h cyclic blue-light illumination. Scale bar: 100 μm. B) Bar chart showing the average percentage of BrdU-positive HSCs. Kruskal–Wallis test followed with multiple comparisons by Dunn's test, $*p < 0.05$, $n = 4$. C) Wound healing assays demonstrating that the gap area covered by migrating HSCs with light-activated TrkA (OptoTrkA-light) is larger than other control groups at 12 and 24h. Scale bar: 100 μm. D) Line graph showing the percentage of the gap area covered by migrating HSCs during the wound healing assay. Kruskal–Wallis test followed with multiple comparisons by Dunn's test, $*p < 0.01$, $**p < 0.01$, $n = 10$. E) Bar chart showing that the average distance of each cell to its nearest neighbor in the OptoTrkA-light group is longer when compared to the cells in other control groups. Kruskal–Wallis test followed with multiple comparisons by Dunn's test, $**p < 0.01$, $n = 10$.

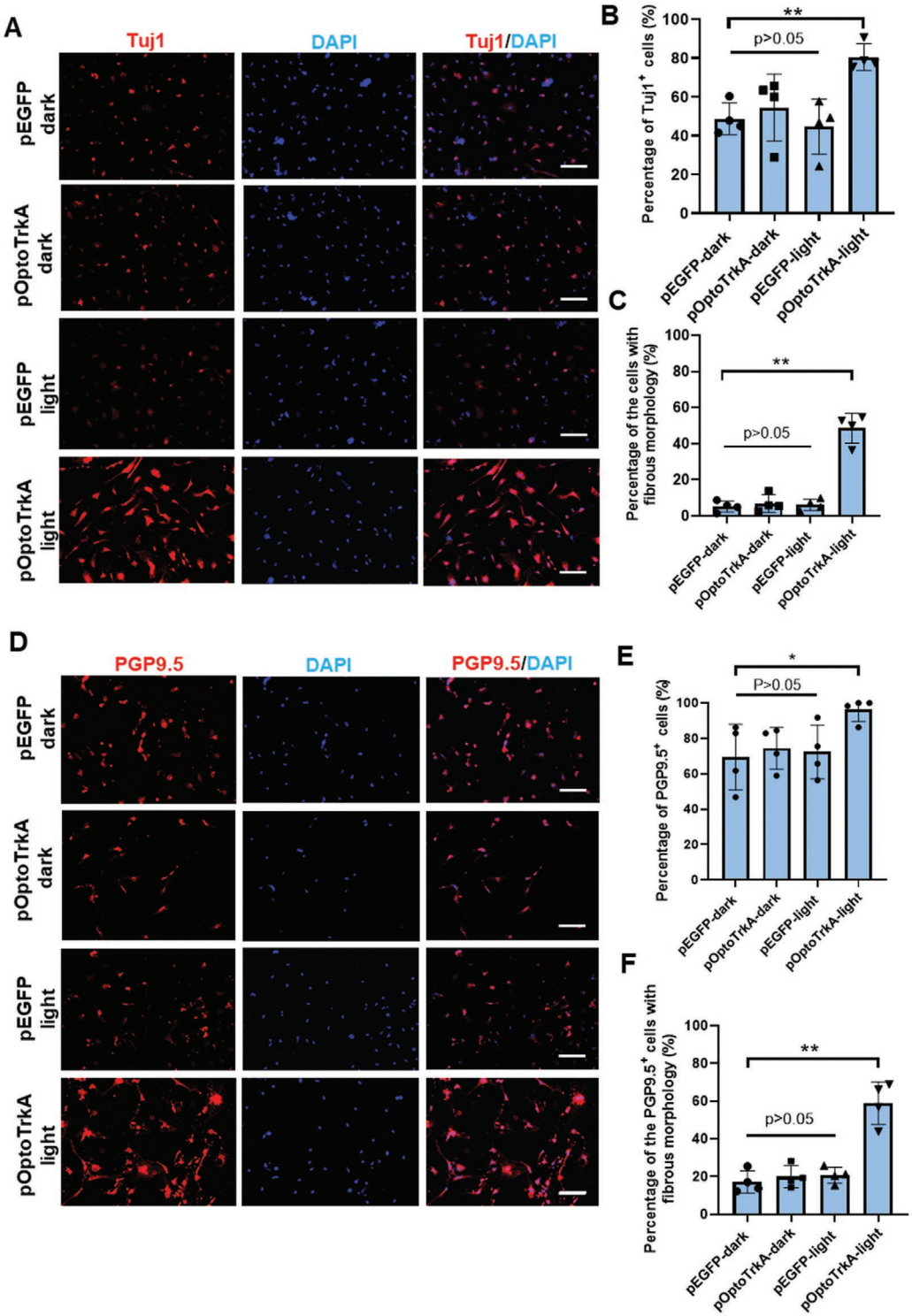

Figure 4. Light-induced activity of OptoTrkA promotes neuronal cell differentiation of HSCs. A) Photomicrographs showing Tuj1 immunofluorescence staining of the neuronal-differentiated HSCs with and without OptoTrkA activity. Scale bar: 100 µm. B) A bar chart showing the percentage of Tuj1 immunoreactive cells. Kruskal–Wallis test followed with multiple comparisons by Dunn's test, $^{**}p < 0.01$, $n = 4$. C) Bar chart showing the percentage of the cells with fibrous morphology among Tuj1 immunoreactive cells. Kruskal–Wallis test followed with multiple comparisons by Dunn's test, $^{**}p < 0.01$, $n = 4$. D) Photomicrographs showing PGP9.5 immunofluorescence staining of neuronal-differentiated HSCs with and without OptoTrkA activity. Scale bar: 100 µm. E) Bar chart showing the percentage of PGP9.5 immunoreactive cells. Kruskal–Wallis test followed with multiple comparisons by Dunn's test, $^{*}p < 0.01$, $n = 4$. F) Bar chart showing the percentage of the cells with fibrous morphology among PGP9.5 immunoreactive cells ($n = 4$). Kruskal–Wallis test followed with multiple comparisons by Dunn's test, $^{**}p < 0.01$, $n = 4$. The relative quantifications are normalized to the leftmost group (as control) and compared between each group for significance analysis.

5. Light-Induced Activation of OptoTrkA Can Enhance Glial Cell Differentiation of HSCs

Next, we sought to further understand if the light-induced activation of OptoTrkA could also promote glial cell differentiation of HSCs. A similar protocol to our neuronal cell differentiation protocol was used, but differentiation was induced by using a glial cell induction medium. In these experiments, we found that HSCs with activated OptoTrkA showed a significantly higher percentage of glial differentiation as determined by immunofluorescence staining of Fabp7 (**Figure 5**A,B) and S100b (Figure 5D,E), but not of GFAP (an astrocyte marker, Figure 1C,D, Supporting Information). In addition, higher fluorescence intensity of Fabp7, S100b, and GFAP was detected in the HSCs with activated OptoTrkA as compared with those in the control groups (Figure 5C,F and Figure 1E, Supporting Information). In conclusion, light-activated OptoTrkA was able to enhance the glial cell differentiation of primary cultured HSCs.

6. OptoTrkA Can be Stimulated by Blue-Light Exposure and Spontaneous Deactivated in the Dark

To interrogate whether OptoTrkA is only activated by blue-light exposure, we performed Western blotting to examine the phosphorylation of downstream signaling pathways regulated by TrkA, including ERK and AKT protein. We transfected the OptoTrkA protein expression plasmid (pOptoTrkA) into HEK293T cells in vitro and stimulated OptoTrkA activity by using blue-light illumination cycles for 12 h (0.2 mW cm^{-2}) (**Figure 6**A). Along the treatment group (pOtpoTrkA-light), three control groups were set up: cells infected with pEGFP-N1 vector and maintained in the dark (pEGFP-dark), cells infected with pOptoTrkA plasmid and maintained in the dark (pOptoTrkA-dark), and cells infected with pEGFP-N1 and illuminated with blue light (pEGFP-light). Western blotting showed that blue-light-stimulated optogenetic TrkA led to increased phosphorylation of ERK1/2 (p-Thr202/Try204) and AKT (p-Ser473) in HEK293T cells, however, illumination of EGFP only controls or OptoTrkA without illumination did not have a significant effect on activating ERK and AKT signaling pathways (Figure 6B–D).

Thereafter, the four experimental groups were all equally placed into the dark for another 24 h to spontaneously deactivate OptoTrkA stimulation. Phosphorylation of ERK1/2 and AKT was determined again by Western blotting. No significant differences in p-ERK1/2 and p-AKT could be detected in the OptoTrkA-light cells when compared to that in the other three control groups which did not have both pOptoTrkA and prior illumination (Figure 6E–G). Taken together, this data suggests that OptoTrkA can be stimulated to activate downstream ERK and AKT signal pathways using blue-light illumination, and this can be spontaneously converted back to an inactivated state when placed into the dark.

7. Discussion

The overall goal of this study is to determine whether stimulation of TrkA activity controlled by blue-light illumination is able to improve cell proliferation, differentiation, and neural differentiation of HSCs. Toward this goal, we developed an optogenetic tool to stimulate TrkA activity in HSCs and deciphered the function of TrkA in these somatic stem cells. We found that light-induced activation of OptoTrkA was able to promote the proliferation of HSCs, which suggests that manipulation of TrkA activation in HSCs has the potential to improve cell survival and increase the population size of cell grafts after transplantation. Second, HSCs with OptoTrkA activity also showed enhanced migratory ability, which has the effect of improving cell grafts colonization in transplant recipient tissue where there is a need to regenerate neurons in large areas or across long distances. Third, HSCs with activated OptoTrkA demonstrated a significantly accelerated neural differentiation toward neuronal and glial lineages. These results suggest that stimulating TrkA activity using optogenetic tools in HSCs is a viable therapeutic strategy to regenerate neural defects in future clinical applications.

TrkA, together with TrkB, TrkC, and $p75^{NTR}$, participate in mediating neurotrophin (NT) signaling. Of the traditional neurotrophic factors, NGF binds TrkA, BDNF and NT-4/5 binds to TrkB, NT-3 binds to TrkC, though all neurotrophic factors are also able to bind to low-affinity neurotrophin receptor $p75^{NTR}$.[11,25,26] The downstream pathways from Trk receptors share many common protein substrates such as the Ras/Mapk/Erk, PLCγ, and PI3K/AKT signaling pathways.[24,25] To our present knowledge, ERK1/2 plays a key role in neuronal survival and axonal maintenance after neural damage,[27,28] and the AKT signaling pathway controls cytoskeletal dynamics for axon elongation and cell migration during neural regeneration.[14,29,30] We found that OptoTrkA is able to significantly activate both ERK1/2 and AKT pathways, which we determined using phosphorylation of ERK1/2 (p-Thr202/Try204) and AKT (p-Ser473) in our Western blotting assay (Figure 3). Previous studies by our group and others have shown that two tyrosine residues, Y490 and Y785, which are located within the intracellular domain of TrkA, serve as the primary phosphorylated sites for triggering downstream ERK1/2, AKT, and PLCγ activation during neuronal differentiation in PC12 cells.[18,31,32] However, even though the functional mechanism of TrkA in HSCs still remains unclear, similar molecular interactions in PC12 may also exist in HSCs. Therefore, specific phosphorylation inhibitors such as U0126 which targets ERK1/2 and LY294002 which targets AKT may help to interrogate the detailed protein–protein interactions during TrkA activation in HSCs and can be used for further studies.

Multipotent stem cells isolated from hair and skin have been successfully used for cell-transplantation therapy in spinal cord-injured and neonatal shivered mice.[33–35] High-throughput profiling by RNA sequencing showed that the neural progenitors from both rodent and human hair follicles have gene expression signatures similar to those of the mouse neural crest stem cells and human neuronal cells.[36,37] HSCs, therefore, are a good target for further studies into genetic modifications and clinical applications in regenerative medicine toward repairing

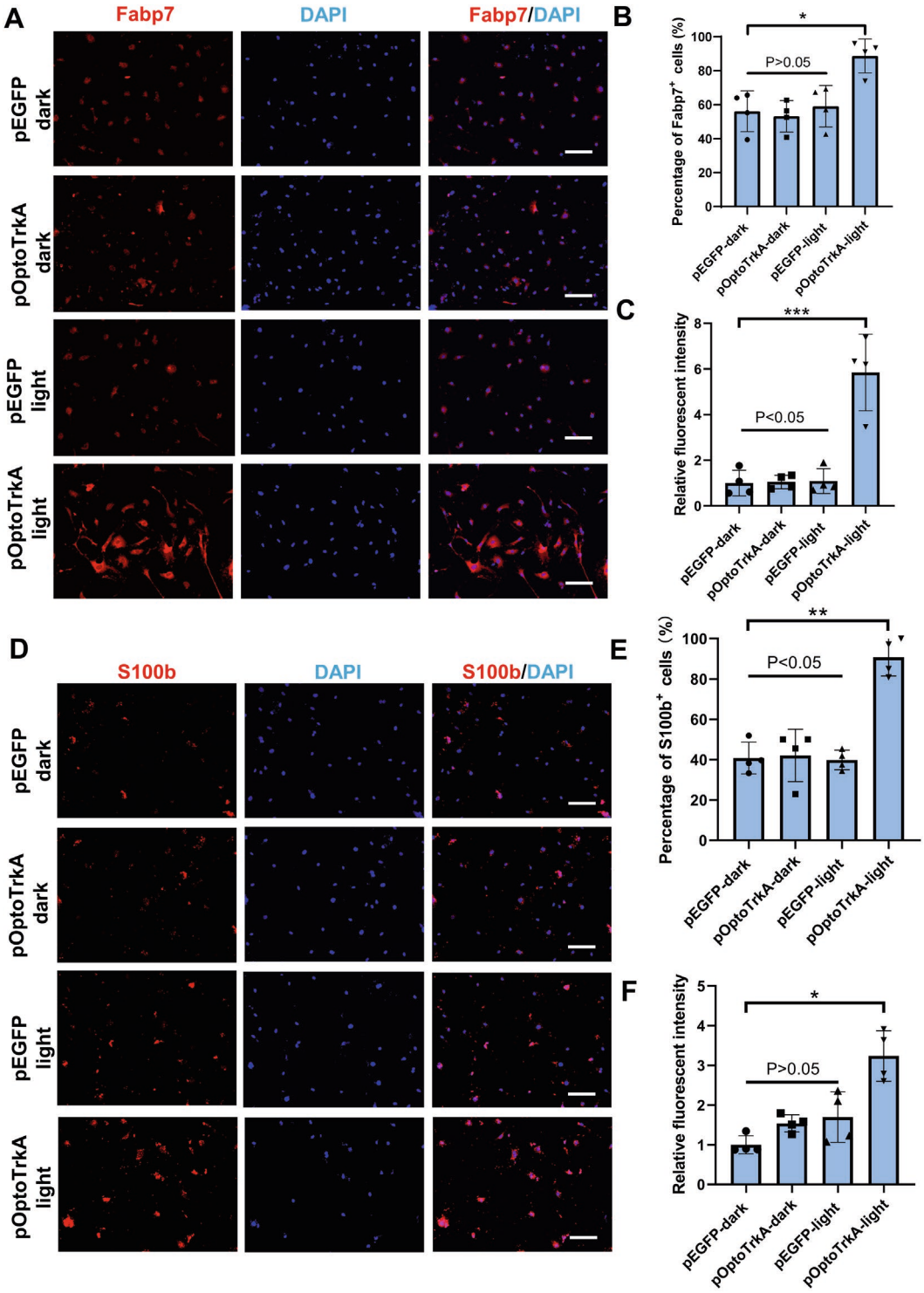

Figure 5. Light-induced activity of OptoTrkA promotes glial cell differentiation of HSCs. A) Photomicrographs showing Fabp7 immunofluorescence staining of glial-differentiated HSCs with and without OptoTrkA activity. Scale bar: 100 µm. B) Bar chart showing the percentage of Fabp7 immunoreactive cells. Kruskal–Wallis test followed with multiple comparisons by Dunn's test, $*p < 0.01$, $n = 4$. C) Bar chart showing the relative immunofluorescence intensity of Fabp7 normalized to DAPI. Kruskal–Wallis test followed with multiple comparisons by Dunn's test, $***p < 0.01$, $n = 4$. D) Photomicrographs showing S100b immunofluorescence staining of glial-differentiated HSCs with and without OptoTrkA activity. Scale bar: 100 µm. E) Bar chart showing the percentage of S100b immunoreactive cells. Kruskal–Wallis test followed with multiple comparisons by Dunn's test, $**p < 0.01$, $n = 4$. F) Bar chart showing the relative immunofluorescence intensity of S100b normalized to DAPI. Kruskal–Wallis test followed with multiple comparisons by Dunn's test, $*p < 0.01$, $n = 4$. The relative quantifications are normalized to the leftmost group (as control) and compared between each group for significance analysis.

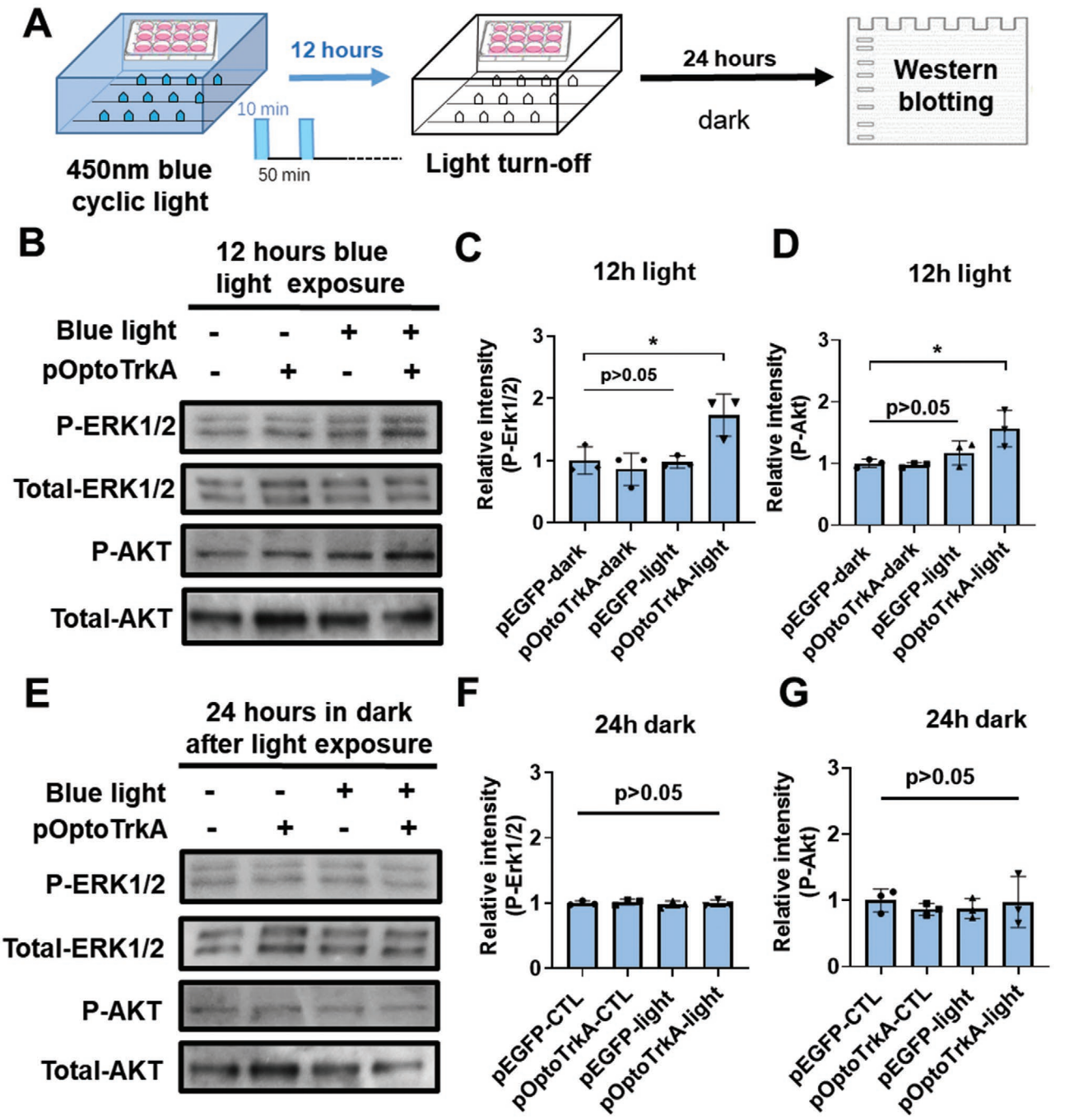

Figure 6. Light-induced OptoTrkA activation increased the phosphorylation of ERK1/2 and AKT. A) OptoTrkA-transfected HEK293T cells and control cells were cultured in a 12-well plate which was placed on an LED light box. Light illumination was set to a 10-min-on, 50-min-off cycle. B) Western blotting showed that cells with OptoTrkA transfection display increased phosphorylation of ERK1/2 and AKT activation when exposed to blue light for 12 h. C,D) Bar charts demonstrate quantifications of relative intensities of the Western blotting in (B). Kruskal–Wallis test followed with multiple comparisons by Dunn's test, $*p < 0.01$, $n = 3$. E) Western blotting showed that cells with OptoTrkA transfections display no significant difference compared to controls when continuously illuminated with cyclic blue light for 12 h and placed in the dark for another 24 h. F,G) Bar charts demonstrate quantifications of relative intensities of the Western blotting in (E). Kruskal–Wallis test, $p > 0.05$, $n = 3$. Quantifications of Western blots are first normalized to the extreme left group (controls) and compared to each group for significance analysis.

neural defects. Enlightened by the previous findings that show that Trk receptor activation can significantly increase the survival rate and neural regeneration efficiency in stromal cell transplantation,[13–15,23] we activated TrkA in HSCs and determined that modulating TrkA activity has beneficial roles in improving proliferation, migration, and neural differentiation.

Table 1. Primers sequences.

Gene name	Forward (5′-3′)	Reverse (5′-3′)
Gapdh	CGTCCCGTAGACAAAATGGT	TTGATGGCAACAATCTCCAC
Oct4	CTTTCCCTCTGTTCCCGTCACTGCTCTG	ATGATGAGTGACAGACAGGCCAGGCTCC
Sox2	TGGTTACCTCTTCCTCCCACTCCAG	AGTTCGCAGTCCAGCCCTCACAT
Nanog	AGGGTCTGCTACTGAGATGCTCTG	CAAACCACTGGTTTTTCTGCCACCG
Nes (Nestin)	GGAGGACCAGAGGATTGTGAACC	ACTGCCATCTGCTCATTCCCTAC
Sox9	GTTGTGGAGGGTTTTAGTTTAGATA	AAAAAAAACTCAACCAAAAATAAATAATA
Sox10	CACTCTGATCCTTTCTCC	GATTGCCTCTGACTCTTT
Nfgr ($p75^{NTR}$)	ACACTGAGCGCCAGTTACG	CTGGGTGCTGGGTGTTGT

As Trk signaling has previously been identified in various solid tumors,[16,17] we used a cautious approach to stimulate TrkA activity via optogenetic tools which are only active during light illumination to effectively reduced the long-term tumorigenic risk. Moving this approach to the clinic is aided by the fact that novel nanometer materials to facilitate deep-tissue light delivery have seen significant improvement in the last decade.[38–40] Therefore, in vivo investigation of TrkA activation in HSCs by optogenetic control for regenerating neurons is a viable next step in improving neural regeneration after transplantation.

8. Conclusion

In conclusion, we have provided evidence that shows that TrkA activation promotes cell proliferation, migration, and neural differentiation of stem cells isolated from the bulge region of mouse vibrissa hair follicle. In addition, with optogenetic tools, TrkA signaling activity can be precisely controlled by blue-light illumination. It is hoped that our work will bring a novel angle to cell-transplantation therapy using somatic stem cells for neural regeneration.

9. Experimental Section

Animals: Wild-type C57BL/6J mice were purchased from the Jackson Laboratory. All mice were maintained on an artificial 12/12 h light/dark cycle. Ethical approval for all animal procedures was obtained from the Sun Yat-sen University Institutional Animal Care and Use Committee (Approval No. SYSU-IACUC-2020-B0538).

Cell Culture: The adult mice (6–8 weeks) were sacrificed by cervical dislocation. The mouse head was sterilized for 1–2 min in a solution consisting of a 50% hydrogen peroxide and a 5% povidone-iodine solution. The whisker pads were dissected and immersed in 1 × Dulbecco's phosphate-buffered saline. The vibrissa hair follicles from the whisker pads were then further dissected by removing the hair dermis, the papilla sebaceous gland, and the connective tissue capsule. A single explant containing HSCs was cultured in α-MEM medium (Gibco, 32571) containing 10% fetal bovine serum (FBS) (Gibco, 16000044). Coverslips for explant culture were coated with 20 μg mL^{-1} collagen type I (BD,354236). After 3 days in culture, the hair follicle explants were removed and emigrated HSCs were further

Table 2. List of antibodies.

Antibody target	Species	Supplier and Cat. No.	Dilution
Nestin	Mouse	Millipore, MAB353	1:500
$p75^{NTR}$	Rabbit	Abcam, ab52987	1:300
Sox10	Rabbit	Abcam, ab27655	1:300
Oct4	Rabbit	Santa Cruz, sc-9081	1:500
Tuj1	Rabbit	Biolegend, 802001	1:500
PGP9.5	Guinea pig	Abcam, ab10410	1:500
Fabp7	Rabbit	Abcam, ab32423	1:300
S100b	Mouse	BD, BD612376	1:500
BrdU	Mouse	Roche, 11170376001	1:500
Erk1/2	Rabbit	CST, 9102	1:2000
P-Erk1/2	Rabbit	CST, 9101	1:2000
Akt	Rabbit	CST, 9272	1:2000
P-Akt	Rabbit	CST, 4060	1:2000
Donkey anti-mouse-Alexa Fluor 488/555	Donkey	Invitrogen, A21202/A31570	1:300
Donkey anti-rabbit-Alexa Fluor 488/555	Donkey	Invitrogen, A21202/A31570	1:300
Goat anti-rabbit-Alexa Fluor 555	Goat	Invitrogen, A21435	1:300
Goat anti-rabbit-HRP	Goat	Invitrogen, 656120	1:10 000

cultured in cell expansion medium which contains DMEM/F12 (Gibco, 1133032), 10% FBS, 1 × B27 supplement, 10 ng mL^{-1} fibroblast growth factor (Gibco, PHG0266-25), epidermal growth factor (EGF) (Gibco, PHG0311), glial-cell-derived neurotrophic factor (R&D System, 212-GD). Primary cultured HSCs were dissociated and passaged using Accutase (Millipore, SCR005) on Day 7. Cell identity was characterized by reverse-transcriptional PCR with the primers listed in **Table 1**.

Differentiation Tests: To induce the differentiation of HSCs into neuronal cells, the cells were transferred to a modified neuronal differentiation medium containing DMEM/F12, 1 × B27 supplement (Gibco, 17504-044), 1 × N2 supplement (Gibco,17502-048), 20 ng mL^{-1} BMP2 (Gibco, PHC7145), and 1 μM all-trans-retinoic acid (Sigma, R2625) for 3 days. To induce differentiation of HSCs into glial cells, the cells were transferred to a modified glial differentiation medium containing DMEM/F12, 2 mM L-glutamine (Gibco, 25030081), 2 ng mL^{-1} insulin (Sigma, I1882), 1 × B27 supplement (Gibco, 17504-044), 1 × N2 supplement (Gibco, 17502-048), and 50 ng mL^{-1} BMP2 (Gibco, PHC7145) for 3 days.

Plasmid Construction and Transfection: The OptoTrkA plasmid was constructed as previously described.[18] Cells were transfected using Lipofectamine Stem Transfection Reagent (Invitrogen, STEM00008) following the manufacturer's instructions. Successful transfection was confirmed by fluorescence microscopy 24 h post-transfection.

Light Stimulation: The instrument used for blue-light illumination was described previously.[18] To stimulate TrkA activity using blue light in HSCs, a 12-well plate containing OptoTrkA-transfected cells was illuminated on a 10/50 min on/off cycle. The light intensity was adjusted to 0.2 mW cm^{-2} at the position of the cells.

Immunofluorescent Staining and Western Blotting: Cells grown on collagen type I-coated coverslips were fixed with 4% paraformaldehyde for 15min at room temperature followed by three rounds of PBS rinsing at 10 min each, The cells were then blocked using 1% BSA (Sigma, 9418) in PBS containing 1% Triton X-100 (USB, 22686) for 1 h. Primary antibodies (**Table 2**) were diluted at the manufacturer's recommended dilution ratio in blocking buffer and incubated with the cells at 4 °C overnight. Secondary antibodies were diluted at a ratio of 1:300 in blocking buffer for 1 h at room temperature. After washing three times in PBS containing 0.5% Tween-20 (USB, 20605), cells were counterstained with 0.15% w/v DAPI (Sigma, 9542) in PBS and mounted using FluorSave Reagent (Millipore, 345789). Fluorescent images were photographed using an epifluorescence microscope (Olympus). For BrdU assays, BrdU reagent was added into culture medium 2 h prior to fixation, after which genomic DNA was denatured using 2 N HCl for 30 min at room temperature to expose BrdU-labeled DNA before following standard immunostaining protocols. For Western blotting, cells were lysed in RIPA buffer (CST, 9806) containing PMSF (Sigma, 10837091001) and cOmplete Protease Inhibitor Cocktail (Roche, 11697498001) on ice for 10 min, followed by centrifugation at 12 000 × *g* for 10 min to remove the insoluble fraction. Protein concentration was measured using the BCA kit (Pierce, 23227). Protein samples were then equalized by dilution in SDS sample buffer and then boiled at 99°C for 5 min before SDS-PAGE. Samples on the acrylamide gel were transferred to activated PVDF membranes (Bio-Rad, 162–0184) and immunoblotted using primary antibodies diluted in 5% BSA:TBST at a ratio of 1:1000, followed by appropriate HRP-conjugated secondary antibodies (diluted at 1:10 000), and finally developed by using the Clarity Western ECL substrate (Bio-Rad, 170–5060).

Wound Healing and Cell Dispersion Assay: A cell-free area for wound healing assay was created by physical exclusion using a commercialized culture insert (ibidi, 81176) following the manufacturer's protocol. To avoid interference from cell proliferation, cells were starved in serum-free DMEM/F12 medium. Images of all groups were taken at 12, 24, and 36 h. At the 12 h time point, cells that migrated into the cell-free area in each group were selected for the cell dispersion assay by measuring the distance of each cell to its closest neighbor.

Statistical Analysis: The ImageJ software was used for image analysis, including the quantification of cell distance, cell number, and fluorescence intensity. All quantitative results were displayed as the mean ± S.D. Statistical significance was assessed using non-parametric ANOVA (Kruskal–Wallis with Dunn's multiple comparisons post-test) using Prism 7 (GraphPad). Statistical significance was set at $p < 0.05$ with a 95% confidence interval.

Supporting Information

Supporting Information is available from the Wiley Online Library or from the author.

Acknowledgements

This work was supported by grants from the National Nature Science Foundation of China (NSFC 81971309), Guangdong Basic and Applied Basic Research Foundation (2019A1515011333), and the Fundamental Research Funds for the Central Universities (F7201931620002).

Conflict of Interest

The authors declare no conflict of interest.

Author Contributions

T.H.: conceptualization, methodology, visualization, investigation, writing—original draft. Y.Z. and Z.W.: visualization. Y.Z.: editing. N.W.: visualization, investigation. H.F.: methodology. Z.H., Y.S., and X.H.: investigation. H.C.: validation. K.Z.: supervision, methodology. C.Y.: supervision, writing—review and editing.

Keywords

hair-follicle-derived stem cells, migration, neuronal and glial differentiation, optogenetically controlled TrkA activity, proliferation

Received: May 20, 2020
Revised: August 19, 2020
Published online:

[1] S. Yi, Y. Zhang, X. K. Gu, L. Huang, K. R. Zhang, T. M. Qian, X. S. Gu, *Burns Trauma* **2020**, *8*, tkaa002.
[2] H. Atkins, *JAMA* **2019**, *321*, 153.
[3] T. K. Watanabe, *PM&R* **2018**, *10*, S151.
[4] Z. B. Jin, M. L. Gao, W. L. Deng, K. C. Wu, S. Sugita, M. Mandai, M. Takahashi, *Prog. Retin. Eye Res.* **2019**, *69*, 38.
[5] K. M. Haston, S. Finkbeiner, *Annu. Rev. Pharmacol.* **2016**, *56*, 489.
[6] F. A. Khan, D. Almohazey, M. Alomari, S. A. Almofty, *Stem Cells Int.* **2018**, *2018*, 1429351.
[7] M. Call, E. A. Meyer, W. W. Kao, F. E. Kruse, U. Schlotzer-Schrehardt, *Bio-Protoc.* **2018**, *8*, e2848.
[8] A. Owczarczyk-Saczonek, M. Krajewska-Wlodarczyk, A. Kruszewska, L. Banasiak, W. Placek, W. Maksymowicz, J. Wojtkiewicz, *Stem Cells Int.* **2018**, *2018*, 1049641.
[9] C. G. Gho, T. Schomann, S. C. de Groot, J. H. M. Frijns, M. N. Rivolta, M. H. A. Neumann, M. A. Huisman, *Cytotechnology* **2016**, *68*, 1849.
[10] K. Obara, N. Tohgi, S. Mii, Y. Hamada, N. Arakawa, R. Aki, S. R. Singh, R. M. Hoffman, Y. Amoh, *Sci. Rep.* **2019**, *9*, 9326.
[11] L. M. Maness, A. J. Kastin, J. T. Weber, W. A. Banks, B. S. Beckman, J. E. Zadina, *Neurosci. Biobehav. Rev.* **1994**, *18*, 143.

[12] E. M. Wexler, O. Berkovich, S. Nawy, *Vis. Neurosci.* **1998**, *15*, 211.
[13] S. Pramanik, Y. A. Sulistio, K. Heese, *Mol. Neurobiol.* **2017**, *54*, 7401.
[14] M. G. Zheng, W. Y. Sui, Z. D. He, Y. Liu, Y. L. Huang, S. H. Mu, X. Z. Xu, J. S. Zhang, J. L. Qu, J. Zhang, D. Wang, *Neural Regen. Res.* **2019**, *14*, 1765.
[15] D. A. Castellanos, P. Tsoulfas, B. R. Frydel, S. Gajavelli, J. C. Bes, J. Sagen, *Cell Transplant.* **2002**, *11*, 297.
[16] J. Meldolesi, *Rev. Physiol. Biochem. Pharmacol.* **2018**, *174*, 67.
[17] A. M. Lange, H. W. Lo, *Cancers* **2018**, *10*, 105.
[18] J. S. Khamo, V. V. Krishnamurthy, Q. Chen, J. Diao, K. Zhang, *Cell Chem. Biol.* **2019**, *26*, 400.
[19] B. Kim, M. Z. Lin, *Biochem. Soc. Trans.* **2013**, *41*, 1183.
[20] K. Muller, S. Naumann, W. Weber, M. D. Zurbriggen, *Biol. Chem.* **2015**, *396*, 145.
[21] D. Tischer, O. D. Weiner, *Nat. Rev. Mol. Cell. Bio.* **2014**, *15*, 551.
[22] E. J. Jung, D. R. Kim, *Mol. Cells* **2008**, *26*, 12.
[23] J. Luzuriaga, J. R. Pineda, I. Irastorza, V. Uribe-Etxebarria, P. Garcia-Gallastegui, J. M. Encinas, P. Chamero, F. Unda, G. Ibarretxe, *Cell. Physiol. Biochem.* **2019**, *52*, 1361.
[24] D. R. Kaplan, F. D. Miller, *Curr. Opin. Cell Biol.* **1997**, *9*, 213.
[25] A. Patapoutian, L. F. Reichardt, *Curr. Opin. Neurobiol.* **2001**, *11*, 272.
[26] W. J. Friedman, L. A. Greene, *Exp. Cell Res.* **1999**, *253*, 131.
[27] V. Waetzig, T. Herdegen, *Mol. Cell. Neurosci.* **2005**, *30*, 67.
[28] Y. Tsuda, M. Kanje, L. B. Dahlin, *BMC Neurosci.* **2011**, *12*, 12.
[29] L. Klimaschewski, B. Hausott, D. N. Angelov, *Int. Rev. Neurobiol* **2013**, *108*, 137.
[30] A. Markus, J. Zhong, W. D. Snider, *Neuron* **2002**, *35*, 65.
[31] J. Biarc, R. J. Chalkley, A. L. Burlingame, R. A. Bradshaw, *J. Biol. Chem.* **2013**, *288*, 16606.
[32] A. Obermeier, R. A. Bradshaw, K. Seedorf, A. Choidas, J. Schlessinger, A. Ullrich, *EMBO J.* **1994**, *13*, 1585.
[33] I. A. McKenzie, J. Biernaskie, J. G. Toma, R. Midha, F. D. Miller, *J. Neurosci.* **2006**, *26*, 6651.
[34] Y. Amoh, M. Kanoh, S. Niiyama, K. Kawahara, Y. Sato, K. Katsuoka, R. M. Hoffman, *Cell Cycle* **2009**, *8*, 176.
[35] M. Sieber-Blum, L. Schnell, M. Grim, M. E. Schwab, *FASEB J.* **2006**, *20*, A441.
[36] H. Yu, S. M. Kumar, A. V. Kossenkov, L. Showe, X. W. Xu, *J. Invest. Dermatol.* **2010**, *130*, 1227.
[37] S. Joost, K. Annusver, T. Jacob, X. Y. Sun, T. Dalessandri, U. Sivan, I. Sequeira, R. Sandberg, M. Kasper, *Cell Stem Cell* **2020**, *26*, 441.
[38] S. Chen, X. G. Liu, T. McHugh, *Proc. SPIE* **2019**, *10873*, 679.
[39] Y. W. Zhang, L. Huang, Z. J. Li, G. L. Ma, Y. B. Zhou, G. Han, *ACS Nano* **2016**, *10*, 3881.
[40] K. Huang, Q. Q. Dou, X. J. Loh, *RSC Adv.* **2016**, *6*, 60896.